Mon. Not. R. Astron. Soc. **000**, 000–000 (0000) Printed 4 September 2012 (MN LaTeX style file v2.2)

Modeling the Anisotropic Two-Point Galaxy Correlation Function on Small Scales and Improved Measurements of $H(z)$, $D_A(z)$, and $\beta(z)$ from the Sloan Digital Sky Survey DR7 Luminous Red Galaxies

Chia-Hsun Chuang,[⋆] and Yun Wang
Homer L. Dodge Department of Physics & Astronomy, Univ. of Oklahoma, 440 W Brooks St., Norman, OK 73019, U.S.A.

arXiv:1209.0210v1 [astro-ph.CO] 2 Sep 2012

4 September 2012

ABSTRACT

We present a simple and efficient phenomenological model for the two-dimensional two-point galaxy correlation function that works well over a wide range of scales, from large scales down to scales as small as $15\,h^{-1}$Mpc. Our model incorporates nonlinear effects, a scale-dependent galaxy bias on small scales, and allows the redshift-space distortions to be scale and direction dependent. We validate our model using LasDamas mock catalogs, and apply it to the Sloan Digital Sky Survey (SDSS) DR7 Luminous Red Galaxies (LRGs). Using only the monopole and quadrupole of the correlation function measured from the SDSS DR7 LRGs, we obtain significantly improved measurements on $H(z)$, $D_A(z)$, and $\beta(z)$: $H(z)r_s(z_d)/c = 0.0423 \pm 0.0027$, $D_A(z)/r_s(z_d) = 6.77 \pm 0.17$, and $\beta(z) = 0.348 \pm 0.058$ at $z = 0.35$, using the scale range of $25 < s < 120h^{-1}$Mpc. We expect our model to be useful in tightening dark energy and gravity constraints from the full analysis of current and future galaxy clustering data.

Key words: cosmology: observations, distance scale, large-scale structure of Universe

1 INTRODUCTION

In our quest to solve the mystery of the observed cosmic acceleration (Riess et al. 1998; Perlmutter et al. 1999), galaxy clustering plays an increasingly important role as a probe of both dark energy and gravity, the two main classes of possible explanations for cosmic acceleration. Current data from the Sloan Digital Sky Survey (SDSS) Data Release Seven (DR7) (Abazajian et al. 2009), WiggleZ (Blake et al. 2009), and BOSS (Eisenstein et al. 2011) are allowing us to place very useful constraints on dark energy. The planned space mission Euclid[1] will survey ~ 60 million emission-line galaxies at $0.7 < z < 2$ over 15,000 square degrees (Cimatti et al. 2009; Wang et al. 2010; Laureijs et al. 2011), and provide potentially revolutionary bounds on the nature of cosmic acceleration.

The SDSS data have been analyzed using both the power spectrum method (see, e.g., Tegmark et al. 2004; Hutsi 2005; Padmanabhan et al. 2007; Blake et al. 2007; Percival et al. 2007, 2010; Reid et al. 2010; Montesano et al. 2011), and the correlation function method (see, e.g., Eisenstein et al. 2005; Okumura et al. 2008; Cabre & Gaztanaga 2009; Martinez et al. 2009; Sanchez et al. 2009; Kazin et al. 2010a; Chuang, Wang, & Hemantha 2012; Samushia et al. 2011; Padmanabhan et al. 2012). Although these two methods are simple Fourier transforms of one another, the analysis processes are quite different and the results cannot be converted using Fourier transform directly because of the finite size of the survey volume.

The power of galaxy clustering as a dark energy probe lies in the fact that the Hubble parameter, $H(z)$, the angular diameter distance, $D_A(z)$, can in principle be extracted simultaneously from data through the measurement of the baryon acoustic oscillation (BAO) scale in the radial and transverse directions (Blake & Glazebrook 2003; Seo & Eisenstein 2003; Wang 2006). The inclusion of information from full galaxy clustering goes beyond BAO only, and enables significantly enhanced constraints on $H(z)$ and $D_A(z)$. Most importantly, it allows the measurement of the growth rate of cosmic large scale structure, $f_g(z) = \beta(z)b(z)$ (where $\beta(z)$ denotes the linear redshift-space distortion (RSD) factor (Kaiser 1987), and $b(z)$ denotes galaxy bias), required for using galaxy clustering to test gravity (Guzzo et al. 2008; Wang 2008). While it will be possible to measure $f_g(z)\sigma_8(z)$ (Song & Percival 2009) or $f_g(z)\sigma_m(z)/r_s(z_d)^4$ (Wang 2012) along with $H(z)$ and $D_A(z)$ in a model-independent manner from future data, current data require assumptions (e.g., CMB priors) being made for such measurements. Measuring $H(z)$, $D_A(z)$, and $\beta(z)$ is comparably easier and more straightforward, and provides a stepping stone for future studies.

[⋆] E-mail: chuang@nhn.ou.edu
[1] http://www.euclid-emc.org/

© 0000 RAS

In Chuang & Wang (2011), we made significant improvements in modeling galaxy clustering from previous studies (Okumura et al. 2008; Cabre & Gaztanaga 2009; Kazin et al. 2010b), and succeeded in making the first simultaneous measurements of $H(z)$ and $D_A(z)$ from data, using the full 2D correlation function of a sample of SDSS DR7 LRGs (Eisenstein et al. 2001), and without assuming a dark energy model or a flat Universe. Very recently, Reid et al. (2012) measured $H(z)$, $D_A(z)$, and growth constraints at $z = 0.57$ from the monopole and quadrupole of the 2D 2PCF of the SDSS III Baryon Oscillation Spectroscopic Survey (BOSS) (SDSS DR9) sample of galaxies, assuming CMB priors. Most recently, Xu et al. (2012) measured $H(z)$ and $D_A(z)$ at $z = 0.35$ from the SDSS DR7 LRGs by applying density-field reconstruction to an anisotropic analysis of the BAO peak.

In Chuang & Wang (2012), we extended our method by exploring the use of the multipoles of the correlation function to measure $H(z)$, $D_A(z)$, and $\beta(z)$. The obvious advantage of using multipoles of the correlation function instead of the full 2D correlation function is the reduced number of data points used to obtain similar amount of information.

The proper modeling of RSD is required in order to measure $\beta(z)$ or $f_g(z)$ from galaxy clustering data. Recent work on improving the modeling of RSD include that of Jennings, Baugh, & Pascoli (2011) and Reid & White (2011). In this paper, we focus on the detailed phenomenological modeling of the correlation function on smaller scales, in order to break the degeneracy between $\beta(z)$ and both $H(z)$ and $D_A(z)$, to obtain significantly improved constraints on $\beta(z)$. We use the multipoles of the 2D correlation function for speed and efficiency.

In Section 2, we introduce the galaxy sample used in our study. In Section 3, we describe the details of our new model. In Section 4, we test our model using mock data. In Section 5, we present our improved measurements from SDSS DR7 LRGs. We summarize and conclude in Sec. 6.

2 DATA

The SDSS has observed one-quarter of the entire sky and performed a redshift survey of galaxies, quasars and stars in five passbands $u, g, r, i,$ and z with a 2.5m telescope (Fukugita et al. 1996; Gunn et al. 1998, 2006). We use the public catalog, the NYU Value-Added Galaxy Catalog (VAGC) (Blanton et al. 2005), derived from the SDSS II final public data release, Data Release 7 (DR7) (Abazajian et al. 2009). We select our LRG sample from the NYU VAGC with the flag $primTarget$ bit mask set to 32. K-corrections have been applied to the galaxies with a fiducial model (ΛCDM with $\Omega_m = 0.3$ and $h = 1$), and the selected galaxies are required to have rest-frame g-band absolute magnitudes $-23.2 < M_g < -21.2$ (Blanton & Roweis 2007). The same selection criteria were used in previous papers (Zehavi et al. 2005; Eisenstein et al. 2005; Okumura et al. 2008; Kazin et al. 2010a). The sample we use is referred to as "DR7full" in Kazin et al. (2010a). Our sample includes 87000 LRGs in the redshift range 0.16-0.44.

Spectra cannot be obtained for objects closer than 55 arcsec within a single spectroscopic tile due to the finite size of the fibers. To correct for these "collisions", the redshift of an object that failed to be measured would be assigned to be the same as the nearest successfully observed one. Both fiber collision corrections and K-corrections have been made in NYU-VAGC (Blanton et al. 2005). The collision corrections applied here are different from what has been suggested in Zehavi et al. (2005). However, the effect should be small since we are using relatively large scale which are less affected by the collision corrections.

We construct the radial selection function as a cubic spline fit to the observed number density histogram with the width $\Delta z = 0.01$. The NYU-VAGC provides the description of the geometry and completeness of the survey in terms of spherical polygons. We adopt it as the angular selection function of our sample. We drop the regions with completeness below 60% to avoid unobserved plates (Zehavi et al. 2005). The Southern Galactic Cap region is also dropped.

3 MODELING 2D CORRELATION FUNCTION

In this section, we describe our model which encompasses the linear scale to the nonlinear scale.

3.1 Modeling 2D Correlation Function for Large Scales

We compute the linear matter power spectra, $P_{lin}(k)$, by using CAMB (Lewis, Challinor, & Lasenby 2000). The linear power spectrum can be composed to two parts:

$$P_{lin}(k) = P_{nw}(k) + P^{lin}_{BAO}(k), \qquad (1)$$

where $P_{nw}(k)$ is the no-wiggle or pure CDM power spectrum calculated using Eq.(29) from Eisenstein & Hu (1998) and $P^{lin}_{BAO}(k)$ is the wiggled part defined by the equation itself. The nonlinear damping effect of the wiggled part in redshift space can be well approximated by (Eisenstein, Seo, & White 2007)

$$P^{nl}_{BAO}(k,\mu_k) = P^{lin}_{BAO}(k)\cdot\exp\left(-\frac{k^2}{2k_\star^2}[1+\mu_k^2(2f_g+f_g^2)]\right), \qquad (2)$$

where $k_\star$ could be computed by (Crocce & Scoccimarro 2006; Matsubara 2008)

$$k_\star = \left[\frac{1}{3\pi^2}\int P_{lin}(k)dk\right]^{-1/2}. \qquad (3)$$

The dewiggled power spectrum is

$$P_{dw}(k,\mu_k) = P_{nw}(k) + P^{nl}_{BAO}(k,\mu_k), \qquad (4)$$

μ_k is the cosine of the angle between $\mathbf{k}$ and the line of sight (LOS). Note that Eqs.(1)-(4) are the same as Eq.(2) in Chuang & Wang (2011), except for the addition of the direction-dependent terms in the exponent of the damping factor in Eq.(2), but are somewhat more intuitive.

Next, we include the linear RSD as follows to obtain the galaxy power spectrum in redshift space at large scales (Kaiser 1987):

$$\begin{aligned} P^s_g(k,\mu_k) &= b^2(1+\beta\mu_k^2)^2 P_{dw}(k,\mu_k), & (5)\\ &= P^s_{g,nw}(k,\mu_k) + P^s_{g,BAO}(k,\mu_k), & (6)\end{aligned}$$

where b is the linear galaxy bias. Note that we have defined

$$P^s_{g,nw}(k,\mu_k) = b^2(1+\beta\mu_k^2)^2 P_{nw}(k) \qquad (7)$$

$$P^s_{g,BAO}(k,\mu_k) = b^2(1+\beta\mu_k^2)^2 P^{nl}_{BAO}(k,\mu_k)$$

$$= b^2(1+\beta\mu_k^2)^2 P^{lin}_{BAO}(k)\cdot\exp\left(-\frac{k^2}{2k_\star^2}[1+\mu_k^2(2f_g+f_g^2]\right) (8)$$

Analogous to Eq.(6), the galaxy correlation function can be decomposed into no-wiggle and wiggled parts as follows:

$$\xi^s_{g,dw}(\sigma,\pi) = \xi^s_{g,nw}(\sigma,\pi) + \xi^s_{g,BAO}(\sigma,\pi). \tag{9}$$

While $\xi^s_{g,dw}(\sigma,\pi)$ can be obtained by Fourier-transforming $P^s_g(k,\mu_k)$, doing so involves two-dimensional integrals, and thus is time-consuming and inefficient. Instead, we can Fourier transform each term in Eq.(6) separately, using Legendre polynomial expansions and integral convolutions that only involve one-dimensional integrals.

The no-wiggle galaxy correlation function in redshift space can be computed by Fourier transforming Eq.(7), which gives (Hamilton 1992)

$$\xi^s_{g,nw}(\sigma,\pi) = b^2(\xi^{nw}_0(s)P_0(\mu)+\xi^{nw}_2(s)P_2(\mu)+\xi^{nw}_4(s)P_4(\mu)), \tag{10}$$

where $s = \sqrt{\sigma^2+\pi^2}$, μ is the cosine of the angle between **s** $= (\sigma,\pi)$ and the LOS, and P_l are Legendre polynomials. The multipoles of ξ^{nw} are defined as

$$\xi^{nw}_0(r) = \left(1+\frac{2\beta}{3}+\frac{\beta^2}{5}\right)\xi^{nw}(r), \tag{11}$$

$$\xi^{nw}_2(r) = \left(\frac{4\beta}{3}+\frac{4\beta^2}{7}\right)[\xi^{nw}(r)-\bar{\xi}(r)], \tag{12}$$

$$\xi^{nw}_4(r) = \frac{8\beta^2}{35}\left[\xi^{nw}(r)+\frac{5}{2}\bar{\xi}^{nw}(r)-\frac{7}{2}\bar{\bar{\xi}}^{nw}(r)\right], \tag{13}$$

where β is the linear RSD parameter and

$$\bar{\xi}^{nw}(r) = \frac{3}{r^3}\int_0^r \xi^{nw}(r')r'^2dr', \tag{14}$$

$$\bar{\bar{\xi}}^{nw}(r) = \frac{5}{r^5}\int_0^r \xi^{nw}(r')r'^4dr', \tag{15}$$

where $\xi^{nw}(r)$ is obtained by fourier transforming $P_{nw}(k)$.

The wiggled part of the galaxy correlation function in redshift space, $\xi^s_{g,BAO}(\sigma,\pi)$, is obtained by Fourier transforming Eq.(8). Note that the μ-dependent damping factor in k-sapce in Eq.(8) becomes a Gaussian convolution in configuration space:

$$\xi^s_{g,BAO}(\sigma,\pi) = \int_{-\infty}^{\infty}\xi^\star(\sigma,\pi-x)\,f_\star(x)dx, \tag{16}$$

where $\xi^\star(\sigma,\pi)$ is the Fourier transform of $b^2(1+\beta\mu_k^2)^2P^{lin}_{BAO}(k)\cdot\exp(-\frac{k^2}{2k_\star^2})$, and

$$f_\star(x) = \frac{1}{\sigma_\star\sqrt{\pi}}\exp\left(-\frac{x^2}{\sigma_\star^2}\right), \tag{17}$$

where

$$\sigma_\star^2 = \frac{4f_g+2f_g^2}{k_\star^2}. \tag{18}$$

$\xi^\star(\sigma,\pi)$ can be obtained using Eq. (10)-(15), but replace $\xi^{nw}(r)$ (the Fourier transform of $P_{nw}(k)$) with the Fourier transform of $P^{lin}_{BAO}(k)\cdot\exp(\frac{-k^2}{2k_\star^2})$.

3.2 Modeling 2D Correlation Function for Small Scales

For small scales, we need to model three effects: the nonlinear matter correlation function, the scale-dependent galaxy bias, and the RSD from the random galaxy pairwise velocities. It is well known that the small scale galaxy correlation function is well described by a powerlaw (Peebles 1980). Since the galaxy correlation function is given by $\xi^{nw}(r)$ on small scales, we model the combination of nonlinear matter correlation function and the scale-dependent galaxy bias at small scales by multiplying $\xi^{nw}(r)$ with the following factor

$$b_{nl}(r) = r^{b_AF(r)}, \tag{19}$$

where b_A is a constant. $F(r)$ is a function which is close to 1 for small r and close to 0 when r is large; we choose

$$F(r) = \frac{1}{1+\left(\frac{r}{b_B}\right)^{b_C}}, \tag{20}$$

where we choose $b_B = 30h^{-1}$Mpc and $b_C = 4$; these are motivated by the fact that the galaxy correlation function is a powerlaw at small scales (i.e. $s < 15h^{-1}$Mpc) and the scale-dependent effects (including nonlinear effects and scale-dependent galaxy bias) are negligible at larger scales, $s > 40h^{-1}$Mpc. The overall scale-dependent effects are included when computing the no-wiggle galaxy correlation function by replacing $\xi^{nw}(r)$ with $\xi^{nw}(r)\times b_{nl}(r)$ in applying Eq. (10)-(15). The resultant correlation function is denoted as $\xi^{s,nl}_{g,nw}(\sigma,\pi)$.

We now obtain the 2D correlation function that incorporate nonlinear effects, galaxy bias, and linear RSD:

$$\tilde{\xi}(\sigma,\pi) = \xi^{s,nl}_{g,nw}(\sigma,\pi) + \xi^s_{g,BAO}(\sigma,\pi), \tag{21}$$

where $\xi^s_{g,BAO}(\sigma,\pi)$ is given by Eq.(16).

Next, we convolve the 2D correlation function with the distribution function of random pairwise velocities, $f(v)$, to obtain the final model $\xi(\sigma,\pi)$ (Peebles 1980)

$$\xi(\sigma,\pi) = \int_{-\infty}^{\infty}\tilde{\xi}\left(\sigma,\pi-\frac{v}{H(z)a(z)}\right)f(v)dv, \tag{22}$$

where the random motions are represented by an exponential form (Ratcliffe et al. 1998; Landy 2002)

$$f(v) = \frac{1}{\sigma_v(s',\mu'^2)\sqrt{2}}\exp\left(-\frac{\sqrt{2}|v|}{\sigma_v(s',\mu'^2)}\right), \tag{23}$$

where σ_v is the pairwise peculiar velocity dispersion, $s'^2 = \sigma^2 + (\pi-\frac{v}{H(z)a(z)})^2$ and $\mu' = \frac{1}{s'}(\pi-\frac{v}{H(z)a(z)})$. We find that the 2D correlation functions measured from LasDamas mocks can be well fitted by

$$\sigma_v(s',\mu'^2) = \sigma_{v,0}(1+c_\mu\mu'^2)(1+c_\sigma e^{-\frac{\sigma^2}{0.01}}), \tag{24}$$

where $\sigma_{v,0}$ is the dispersion corresponding to the truly random motion and c_μ and c_σ terms describe the dependence on direction and separation respectively. The σ-dependence is similar to that found by Cabre & Gaztanaga (2009). They found that the 2D correlation functions from the MICE N-body simulations are fitted well with a pairwise velocity distribution which is large when $\sigma < 5h^{-1}$Mpc. We have added the direction-dependent term, $c_\mu\mu'^2$, to model the high amplitude of $\hat{\xi}_4$ at small scales (see Fig. 4).

4 VALIDATION OF THE MODEL USING MOCK CATALOGS

In this section, we present the methodology and results of testing our model described in the previous section.

4.1 Mock Catalogs Used

We use the 160 mock catalogs from the LasDamas simulations[2] (McBride et al., in preparation) to test our model. LasDamas provides mock catalogs matching SDSS main galaxy and LRG samples. We use the LRG mock catalogs from the LasDamas gamma release with the same cuts as the SDSS LRG DR7full sample, $-23.2 < M_g < -21.2$ and $0.16 < z < 0.44$. We have diluted the mock catalogs to match the radial selection function of the observational data by randomly selecting the mock galaxies according to the number density of the data sample. We calculate the multipoles of the correlation functions of the mock catalogs and construct the covariance matrix (see Chuang & Wang (2012) for details).

4.2 Measuring the Two-Dimensional Two-Point Correlation Function

We convert the measured redshifts of galaxies to comoving distances by assuming a fiducial model, ΛCDM with $\Omega_m = 0.25$. We use the two-point correlation function estimator given by Landy & Szalay (1993):

$$\xi(\sigma,\pi) = \frac{DD(\sigma,\pi) - 2DR(\sigma,\pi) + RR(\sigma,\pi)}{RR(\sigma,\pi)}, \tag{25}$$

where π is the separation along the line of sight (LOS), σ is the separation in the plane of the sky, DD, DR, and RR represent the normalized data-data, data-random, and random-random pair counts respectively in a given distance range. The LOS is defined as the direction from the observer to the center of a pair. The bin size we use here is 1 h^{-1}Mpc×1 h^{-1}Mpc. The Landy and Szalay estimator has minimal variance for a Poisson process. Random data are generated with the same radial and angular selection functions as the real data. One can reduce the shot noise due to random data by increasing the number of random data. The number of random data we use is 10 times that of the real data. While calculating the pair counts, we assign to each data point a radial weight of $1/[1 + n(z) \cdot P_w]$, where $n(z)$ is the radial selection function and $P_w = 4 \cdot 10^4\ h^{-3}$Mpc^3 (Eisenstein et al. 2005).

Fig 1 shows the averaged 2D correlation function measured from the mock catalogs. We use the averaged radial selection function to construct the random catalog since it is closer to the true mean density. Clearly, our model provides an excellent fit to data over a wide range of scales, from the largest scales where data are not too noisy, to the smallest scales plotted (except very near the LOS).

4.3 Multiples of the Correlation Function

As in Chuang & Wang (2012), the effective multipoles of the correlation function are defined by

$$\hat{\xi}_l(s) \equiv \frac{\displaystyle\sum_{s-\frac{\Delta s}{2}<\sqrt{\sigma^2+\pi^2}<s+\frac{\Delta s}{2}} (2l+1)\xi(\sigma,\pi)P_l(\mu)\sqrt{1-\mu^2}}{\text{Number of bins used in the numerator}}, \tag{26}$$

where $\Delta s = 5\ h^{-1}$Mpc in this work, and

$$\sigma = (n + \frac{1}{2})h^{-1}\text{Mpc}, n = 0, 1, 2, ... \tag{27}$$

$$\pi = (m + \frac{1}{2})h^{-1}\text{Mpc}, m = 0, 1, 2, ... \tag{28}$$

$$\mu \equiv \frac{\pi}{\sqrt{\sigma^2 + \pi^2}}. \tag{29}$$

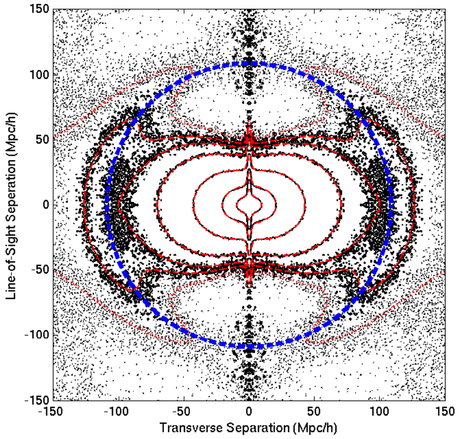

Figure 1. The average two-dimensional two-point correlation function (2D 2PCF) measured from 160 LasDamas SDSS LRGfull mock catalogs (solid black contours), compared to a theoretical model with the input parameters of the LasDamas simulations and $\{\beta$, b_A, $\sigma_{v,0}$, c_μ, $c_\sigma\}$ are set to $\{0.316$, -0.0385, 50km s^{-1}, 10, 4$\}$ (dashed red contours). The thick dashed blue circle denotes the baryon acoustic oscillation scale. The contour levels are $\xi = 2, 0.5, 0.1, 0.025, 0.01, 0.005, 0$. The $\xi = 0$ contours are denoted with dotted lines for clarity.

Note that both the measurements and the theoretical predictions for the effective multipoles are computed using Eq.(26). We do not use the conventional definitions of multipoles to extract parameter constraints as they use continuous integrals. Bias could be introduced if the definitions of multipoles are different between measurements from data and the theoretical model.

Fig. 2, 3, and 4 show the effective monopole ($\hat{\xi}_0$), quadrupole ($\hat{\xi}_2$), and hexadecapole ($\hat{\xi}_4$) measured from the LasDamas mock catalogs comparing to our full model and a simpler model (linear model + 1D dewiggle damping + constant velocity dispersion). In Fig. 2, one can see how our model completely corrects the scale-dependent effects in the measured monopole. Fig.3 shows that our model provides a reasonable fit to the measured quadrupole. In Fig. 4, we find that angle-dependent term, c_σ, significantly improves the fitting of hexadecapole at small scales ($s < 50h^{-1}$Mpc). However, at larger scales($s > 60h^{-1}$Mpc), the LasDamas mocks show some oscillatory features while the theoretical models are flat. It is likely due to the dewiggle damping not being adequate enough to model ξ_4 and one might need higher order term (i.e. μ^4). Therefore, we do not include ξ_4 to measure parameters in this study.

4.4 Covariance Matrix

We construct the covariance matrix as

$$C_{ij} = \frac{1}{N-1}\sum_{k=1}^{N}(\bar{X}_i - X_i^k)(\bar{X}_j - X_j^k), \tag{30}$$

where N is the number of the mock catalogs, $\bar{X}_m$ is the mean of the m^{th} element of the vector from the mock catalog multipoles, and X_m^k is the value in the m^{th} elements of the vector from the k^{th} mock catalog multipoles. The data vector $\mathbf{X}$ is defined by

$$\mathbf{X} = \{\hat{\xi}_0^{(1)}, \hat{\xi}_0^{(2)}, ..., \hat{\xi}_0^{(N)}; \hat{\xi}_2^{(1)}, \hat{\xi}_2^{(2)}, ..., \hat{\xi}_2^{(N)}; ...\}, \tag{31}$$

---

[2] http://lss.phy.vanderbilt.edu/lasdamas/

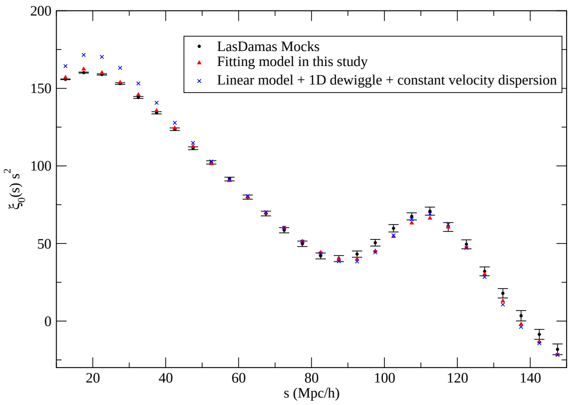

Figure 2. The averaged monopole of the correlation functions of the mock catalogs (black squares) comparing to the fitting model of this study (red dots) and a simpler model (linear model + 1D dewiggle damping + constant velocity dispersion,blue crosses). The error bars are taken as $1/\sqrt{160}$ of the square roots of the diagonal elements of the covariance matrix.

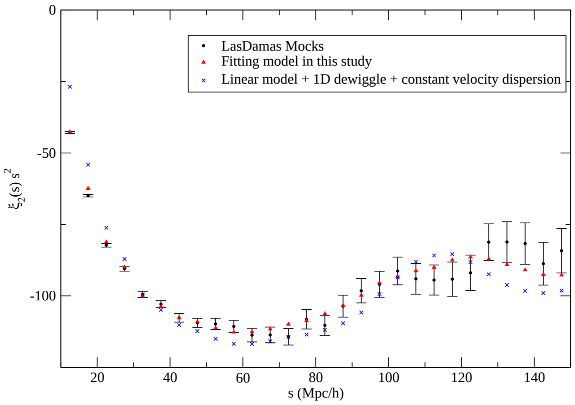

Figure 3. The averaged quadrupole of the correlation functions of the mock catalogs (black squares) comparing to the fitting model of this study (red dots) and a simpler model (linear model + 1D dewiggle damping + constant velocity dispersion,blue crosses). The error bars are taken as $1/\sqrt{160}$ of the square roots of the diagonal elements of the covariance matrix.

where N is the number of data points in each measured multipole; $N = 19$ while using the scale range, $25 < s < 120h^{-1}$Mpc. The length of the data vector $\mathbf{X}$ depends on how many multipoles are used.

4.5 Likelihood

The likelihood is taken to be proportional to $\exp(-\chi^2/2)$ (Press et al. 1992), with χ^2 given by

$$\chi^2 \equiv \sum_{i,j=1}^{N_X} \left[X_{th,i} - X_{obs,i}\right] C_{ij}^{-1} \left[X_{th,j} - X_{obs,j}\right] \tag{32}$$

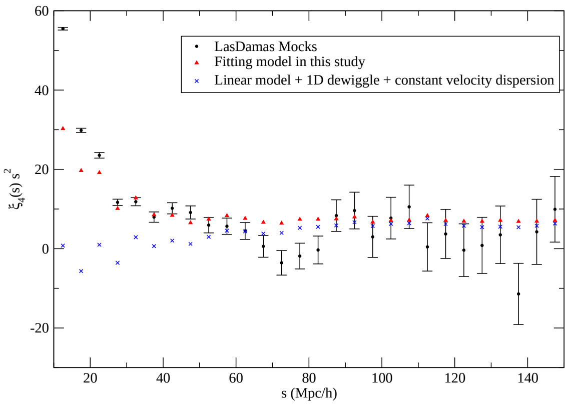

Figure 4. The averaged hexadecapole of the correlation functions of the mock catalogs (black squares) comparing to the fitting model of this study (red dots) and a simpler model (linear model + 1D dewiggle damping + constant velocity dispersion,blue crosses). The error bars are taken as $1/\sqrt{160}$ of the square roots of the diagonal elements of the covariance matrix.

where N_X is the length of the vector used, X_{th} is the vector from the theoretical model, and X_{obs} is the vector from the observational data (we use the mock catalogs as the observational data to test the model in this section).

As explained in Chuang & Wang (2011), instead of recalculating the observed correlation function for different theoretical models, we rescale the theoretical correlation function to avoid rendering χ^2 values arbitrary. The rescaled theoretical correlation function is computed by

$$T^{-1}(\xi_{th}(\sigma,\pi)) = \xi_{th}\left(\frac{D_A(z)}{D_A^{fid}(z)}\sigma, \frac{H^{fid}(z)}{H(z)}\pi\right), \tag{33}$$

where ξ_{th} is given by eq. (22). Hence χ^2 can be rewritten as

$$\begin{aligned}\chi^2 \equiv & \sum_{i,j=1}^{N_X} \left\{T^{-1}X_{th,i} - X^{fid}_{obs,i}\right\} C^{-1}_{fid,ij} \cdot \\ & \cdot \left\{T^{-1}X_{th,j} - X^{fid}_{obs,j}\right\}, \end{aligned} \tag{34}$$

where $T^{-1}X_{th}$ is a vector given by eq. (33) with ξ_{th} replaced by its effective multipoles (defined by eq. (26)), and X^{fid}_{obs} is the corresponding vector from observational data measured assuming the fiducial model in converting redshifts to distances. See Chuang & Wang (2011) for a more detailed description of our rescaling method.

4.6 Markov Chain Monte-Carlo Likelihood Analysis

We use CosmoMC in a Markov Chain Monte-Carlo likelihood analysis (Lewis & Bridle 2002). The parameter space that we explore spans the parameter set of $\{H(0.35),\ D_A(0.35),\ \Omega_m h^2,\ \beta,\ \Omega_b h^2,\ n_s,\ b_A,\ \sigma_{v,0},\ c_\mu,\ c_\sigma\}$. Only $\{H(0.35),\ D_A(0.35),\ \Omega_m h^2,\ \beta\}$ are well constrained by the mock data. We marginalize over $\{b_A,\ \sigma_{v,0},\ c_\mu,\ c_\sigma\}$ with the flat priors, $\{(-0.2, 0.2),\ (0, 500)\mathrm{s}^{-1}\mathrm{km},\ (0, 20),\ (0, 10)\}$. We marginalize the values of $\Omega_b h^2$ and n_s with a wide range ($\pm 7\sigma_{WMAP}$ Komatsu et al. (2010)) centered at the input values of simulations (for mocks) or WMAP7 measurements. We also marginalize over the amplitude of the galaxy correlation function. For simplicity, we fix $f_g(z = 0.35)$ in the asymmetric damping factor in Eq.(2) to the fiducial value, 0.645. Our results are not sensitive to this choice.

4.7 Validation of the Model Using One Mock

To simulate the application of our model to the SDSS DR7 LRGs, we apply it to one LasDamas SDSS LRG mock catalog, to test whether the true values of the parameters (the input parameters) are recovered by our methodology. Table 1 shows the measurements of $\{H(0.35)$, $D_A(0.35)$, $\Omega_m h^2$, β, $H(0.35)\, r_s(z_d)/c$, $D_A(0.35)/r_s(z_d)\}$ from one LasDamas SDSS LRG mock catalog (indexed 01a in the LasDamas simulations). Clearly, when smaller scales are included, the constraints are improved, while the mean values generally become closer to the input values (although there are fluctuations due to sample variance). Finally, we find that χ^2 per degree of freedom is reasonable, and reflects the level of noise and systematic bias inherent in the mock data.

5 IMPROVED MEASUREMENTS FROM SDSS DR7 LRG

Table 2 lists the mean and rms variance of the parameters, $\{H(0.35)$, $D_A(0.35)$, $\Omega_m h^2$, β, $H(0.35)\, r_s(z_d)/c$, $D_A(0.35)/r_s(z_d)\}$, derived in an MCMC likelihood analysis from the measured $\hat{\xi}_0 + \hat{\xi}_2$ of the correlation function of the SDSS LRG sample with the scale range, $25 < s < 120\, h^{-1}$Mpc. Table 3 gives the corresponding normalized covariance matrix.

We do not use smaller scales (i.e. $15 < s < 120\, h^{-1}$Mpc) because it gives a much too high χ^2/d.o.f. (larger than 2). We marginalize over the other parameters, $\{\Omega_b h^2$, n_s, $\sigma_v\}$, with flat priors over the ranges of $\{(0.01859, 0.02657)$, $(0.865, 1.059)$, $(0, 500)\mathrm{s}^{-1}\mathrm{km}\}$, where the flat priors of $\Omega_b h^2$ and n_s are centered on the measurements from WMAP7 and has width of $\pm 7\sigma_{WMAP}$ (with σ_{WMAP} from Komatsu et al. (2010)). These priors are wide enough to ensure that CMB constraints are not double counted when our results are combined with CMB data (Chuang, Wang, & Hemantha 2012). We also marginalize over the amplitude of the galaxy correlation function.

Our model in Chuang & Wang (2012) was only applicable for $40 < s < 120h^{-1}$Mpc. Comparing our results from this study ($25 < s < 120h^{-1}$Mpc) and those from our previous study in Chuang & Wang (2012) ($40 < s < 120h^{-1}$Mpc) in Table 2, one can see the dramatic improvement in the constraints obtained from this study from adding the information on smaller scales.

It is important to note that the correlation between $\beta(0.35)$ and $\{H(0.35)r_s(z_d)/c$, $D_A(0.35)/r_s(z_d)\}$ are significantly reduced: $r(\beta(0.35), H(0.35)r_s(z_d)) = 0.748$ and $r(\beta(0.35), D_A(0.35)/r_s(z_d)) = 0.575$ for $40 < s < 120h^{-1}$Mpc (Chuang & Wang 2012), versus $r(\beta(0.35), H(0.35)r_s(z_d)) = 0.494$ and $r(\beta(0.35), D_A(0.35)/r_s(z_d)) = 0.159$ for $25 < s < 120\, h^{-1}$Mpc (this study).

	$25 < s < 120$	$40 < s < 120$
$H(0.35)$	76.3 ± 5.6	79.6 ± 8.8
$D_A(0.35)$	1126 ± 49	1060 ± 92
$\Omega_m h^2$	0.097 ± 0.012	0.103 ± 0.015
β	0.348 ± 0.058	0.44 ± 0.15
$H(0.35)\, r_s(z_d)/c$	0.0423 ± 0.0027	0.0435 ± 0.0045
$D_A(0.35)/r_s(z_d)$	6.77 ± 0.17	6.44 ± 0.51
χ^2/d.o.f.	1.65	1.23

Table 2. The mean and standard deviation of $\{H(0.35)$, $D_A(0.35)$, $\Omega_m h^2$, β, $H(0.35)\, r_s(z_d)/c$, $D_A(0.35)/r_s(z_d)\}$ from SDSS DR7 LRGs using $\hat{\xi}_0 + \hat{\xi}_2$ and the scale range, $25 < s < 120h^{-1}$Mpc, comparing with the measurements from our previous paper (Chuang & Wang 2012) using only large scales, $40 < s < 120h^{-1}$Mpc. The χ^2/d.o.f. is 1.65 which is a bit high but still could be due to the sample variance. The unit of H is $\mathrm{km\,s^{-1}\,Mpc^{-1}}$. The unit of D_A and $r_s(z_d)$ is Mpc.

6 CONCLUSION AND DISCUSSION

We have presented and validated a simple and efficient phenomenological model for the two-dimensional two-point galaxy correlation function that works well over a wide range of scales, from large scales down to small scales not used in our previous work (where we restricted ourselves to scales larger than $40\, h^{-1}$Mpc). Applying this model to the SDSS LRGs over the scale range of $25 < s < 120h^{-1}$Mpc, we are able to break the degeneracy between $\beta(z)$ with both $H(z)$ and $D_A(z)$, and obtain significantly improved measurements: $H(z)r_s(z_d)/c = 0.0423 \pm 0.0027$, $D_A(z)/r_s(z_d) = 6.77 \pm 0.17$, and $\beta(z) = 0.348 \pm 0.058$ at $z = 0.35$.

Our model incorporates the overall nonlinear effects via the use of the "dewiggled" galaxy power spectrum, as in Chuang & Wang (2011), but we now include the enhanced damping along the line of sight (see Eqs.(1)-(4)), even though it only has a small effect on the results. On small scales, the nonlinear effect and scale-dependent galaxy bias are degenerate, and we model these as an overall scale-dependent correction. Most significantly, we allow the RSD to be scale and direction dependent in our model. Our model provides excellent fit to mock data (see Fig.1).

In order to test our model in a timely fashion, we have chosen to use only the monopole and quadrupole of the 2D correlation function, instead of the full 2D correlation function, in our analysis of the mock and real data. While our model provides an excellent fit to mock data down to a scale of $15\, h^{-1}$Mpc, it leads to a steep increase in the χ^2 per degree of freedom at scales smaller than 25 h^{-1}Mpc when applied to the SDSS DR7 LRGs. However, the constraints on $H(z)r_s(z_d)$, $D_A(z)/r_s(z_d)$, and $\beta(z)$ remain consistent at the 68% C.L., while the errors on these increase as we include scales below 25 h^{-1}Mpc. This may indicate that the full 2D correlation function (instead of just its monopole and the quadrupole) needs to be used to model the data on smaller scales. We will do so in our future work. We will apply our model to the public BOSS data, which will allow a greater range of scales (on both small and large scales) to be used in the analysis for measuring $H(z)r_s(z_d)$, $D_A(z)/r_s(z_d)$, and $\beta(z)$.

We expect our model to be useful in tightening dark energy and gravity constraints from the full analysis of current and future galaxy clustering data.

ACKNOWLEDGEMENTS

We are grateful to the LasDamas project for making their mock catalogs publicly available. The computing for this project was performed at the OU Supercomputing Center for Education and Research (OSCER) at the University of Oklahoma (OU). This work used the Extreme Science and Engineering Discovery Environ-

	$15 < s < 120$	$25 < s < 120$	$30 < s < 120$	$40 < s < 120$	input value
$H(0.35)$	86 ± 11	78 ± 13	79 ± 12	83 ± 13	81.79
$D_A(0.35)$	1050 ± 92	1003 ± 112	1008 ± 110	1035 ± 116	1032.8
$\Omega_m h^2$	0.125 ± 0.018	0.115 ± 0.017	0.114 ± 0.018	0.116 ± 0.019	0.1225
β	0.41 ± 0.12	0.44 ± 0.15	0.50 ± 0.16	0.57 ± 0.17	–
$H(0.35)\, r_s(z_d)/c$	0.0457 ± 0.0052	0.0423 ± 0.0064	0.0429 ± 0.0062	0.0451 ± 0.0068	0.0434
$D_A(0.35)/r_s(z_d)$	6.59 ± 0.54	6.17 ± 0.67	6.18 ± 0.64	6.36 ± 0.68	6.48
χ^2/d.o.f.	1.24	1.09	1.06	1.03	–

Table 1. The mean and standard deviation of the distribution of the measured values of $\{H(0.35),\ D_A(0.35),\ \Omega_m h^2,\ \beta,\ H(0.35)\, r_s(z_d)/c,$ $D_A(0.35)/r_s(z_d)\}$ from one LasDamas SDSS LRG mock catalog (indexed 01a) using four scale ranges, $15 < s < 120h^{-1}$Mpc, $25 < s < 120h^{-1}$Mpc, $30 < s < 120h^{-1}$Mpc and $40 < s < 120h^{-1}$Mpc. The constraint of β is significantly improved when including smaller scales. The mean value of β is also closer to expected value, ~ 0.32 (see Chuang & Wang (2012)). The unit of the separation, s, is h^{-1}Mpc. The unit of H is $\mathrm{km\,s^{-1}\,Mpc^{-1}}$. The unit of D_A and $r_s(z_d)$ is Mpc.

	$H(0.35)$	$D_A(0.35)$	$\Omega_m h^2$	β	$H(0.35)\, r_s(z_d)/c$	$D_A(0.35)/r_s(z_d)$
$H(0.35)$	1.0000	-0.2788	0.4525	0.4160	0.8625	0.2597
$D_A(0.35)$	-0.2788	1.0000	-0.7617	0.1112	0.1515	0.5092
$\Omega_m h^2$	0.4525	-0.7617	1.0000	-0.0856	-0.0290	0.0869
β	0.4160	0.1112	-0.0856	1.0000	0.4941	0.1594
$H(0.35)\, r_s(z_d)/c$	0.8625	0.1515	-0.0290	0.4941	1.0000	0.2483
$D_A(0.35)/r_s(z_d)$	0.2597	0.5092	0.0869	0.1594	0.2483	1.0000

Table 3. Normalized covariance matrix of the measured and derived parameters, $\{H(0.35),\, D_A(0.35),\, \Omega_m h^2,\, \beta,\, H(0.35)\, r_s(z_d)/c,\, D_A(0.35)/r_s(z_d)\}$ from SDSS DR7 LRGs using $\hat{\xi}_0 + \hat{\xi}_2$ and the scale range, $25 < s < 120h^{-1}$Mpc.

ment (XSEDE), which is supported by National Science Foundation grant number OCI-1053575. This work was supported by DOE grant DE-FG02-04ER41305.

Funding for the Sloan Digital Sky Survey (SDSS) has been provided by the Alfred P. Sloan Foundation, the Participating Institutions, the National Aeronautics and Space Administration, the National Science Foundation, the U.S. Department of Energy, the Japanese Monbukagakusho, and the Max Planck Society. The SDSS Web site is http://www.sdss.org/.

The SDSS is managed by the Astrophysical Research Consortium (ARC) for the Participating Institutions. The Participating Institutions are The University of Chicago, Fermilab, the Institute for Advanced Study, the Japan Participation Group, The Johns Hopkins University, Los Alamos National Laboratory, the Max-Planck-Institute for Astronomy (MPIA), the Max-Planck-Institute for Astrophysics (MPA), New Mexico State University, University of Pittsburgh, Princeton University, the United States Naval Observatory, and the University of Washington.

REFERENCES

Abazajian, K. N., *et al.* [SDSS Collaboration], Astrophys. J. Suppl. **182**, 543 (2009) [arXiv:0812.0649 [astro-ph]].

Alcock, C., and Paczynski, B., Nature **281**, 358 (1979).

Blake, C., Glazebrook, K, 2003, ApJ, 594, 665

Blake, C.; Collister, A.; Bridle, S.; and Lahav, O., Mon. Not. Roy. Astron. Soc. **374**, 1527 (2007) [arXiv:astro-ph/0605303].

Blake, C., et al. 2009, MNRAS, 395, 240

Blanton, M. R., *et al.* [SDSS Collaboration], Astron. J. **129**, 2562 (2005) [arXiv:astro-ph/0410166].

Blanton, M. R.; and Roweis, S., Astron. J. **133**, 734 (2007) [arXiv:astro-ph/0606170].

Cabre, A.; and Gaztanaga, E., Mon. Not. Roy. Astron. Soc. **393**, 1183 (2009) [arXiv:0807.2460 [astro-ph]].

Chuang, C. -H.; Wang, Y.; and Hemantha, M. D. P., Mon. Not. Roy. Astron. Soc. **423**, 1474 (2012) [arXiv:1008.4822 [astro-ph.CO]].

Chuang, C. -H. and Wang, Y. MNRAS, in press, arXiv:1102.2251 [astro-ph.CO].

Chuang, C. -H. and Wang, Y. arXiv:1205.5573 [astro-ph.CO].

Cimatti, A.; Robberto, M.; Baugh, C. M.; Beckwith, S. V. W.; Content, R.; Daddi, E.; De Lucia, G.; and Garilli B.*et al.*, Exper. Astron. **23**, 39 (2009) [arXiv:0804.4433 [astro-ph]].

Crocce, M., and Scoccimarro, R., Phys. Rev. D **73**, 063520 (2006) [arXiv:astro-ph/0509419].

Eisenstein, D. J.; and Hu, W., Astrophys. J. **496**, 605 (1998) [arXiv:astro-ph/9709112].

Eisenstein, D. J., *et al.* [SDSS Collaboration], Astron. J. **122**, 2267 (2001) [arXiv:astro-ph/0108153].

Eisenstein, D. J., *et al.* [SDSS Collaboration], Astrophys. J. **633**, 560 (2005) [arXiv:astro-ph/0501171].

D. J. Eisenstein, H. -j. Seo and M. J. White, 1, Astrophys. J. **664**, 660 (2007) [astro-ph/0604361].

Eisenstein, D.J., et al., 2011, AJ, 142, 72

Fukugita, M.; Ichikawa, T.; Gunn, J. E.; Doi, M.; Shimasaku, K.; and Schneider, D. P., Astron. J. **111**, 1748 (1996).

Gaztanaga, E.; Cabre, A.; and Hui, L. Mon. Not. Roy. Astron. Soc. **399**, 1663 (2009) [arXiv:0807.3551 [astro-ph]].

Gunn, J. E., *et al.* [SDSS Collaboration], Astron. J. **116**, 3040 (1998) [arXiv:astro-ph/9809085].

Gunn, J. E., *et al.* [SDSS Collaboration], Astron. J. **131**, 2332

(2006) [arXiv:astro-ph/0602326].

Guzzo, L., et al., 2008, Nature, 451, 541

Hamilton, A. J. S., 1992, APJL, 385, L5

Hutsi, G., arXiv:astro-ph/0507678.

Jennings, E.; Baugh, C. M.; and Pascoli, S., Mon. Not. Roy. Astron. Soc. **410**, 2081 (2011) [arXiv:1003.4282 [astro-ph.CO]].

Kaiser, N., Mon. Not. Roy. Astron. Soc. **227**, 1 (1987).

Kazin, E. A., *et al.*, Astrophys. J. **710**, 1444 (2010) [arXiv:0908.2598 [astro-ph.CO]].

Kazin, E. A.; Blanton, M. R.; Scoccimarro, R.; McBride, C. K.; and Berlind, A. A., Astrophys. J. **719**, 1032 (2010) [arXiv:1004.2244 [astro-ph.CO]].

Kazin, E. A.; Sanchez, A. G.; and Blanton, M. R. Mon. Not. Roy. Astron. Soc. **419**, 3223 (2012) [arXiv:1105.2037 [astro-ph.CO]].

Komatsu, E. *et al.* [WMAP Collaboration], Astrophys. J. Suppl. **192**, 18 (2011) [arXiv:1001.4538 [astro-ph.CO]].

Landy, S. D. and Szalay, A. S., Astrophys. J. **412**, 64 (1993).

Landy, S. D., “The Pairwise Velocity Distribution Function of Galaxies in the LCRS, 2dF, Astrophys. J. **567**, L1 (2002) [arXiv:astro-ph/0202130].

Laureijs, R., et al., “Euclid Definition Study Report”, arXiv:1110.3193

Lewis, A.; Challinor, A.; and Lasenby, A., Astrophys. J. **538**, 473 (2000) [arXiv:astro-ph/9911177].

Lewis, A. and Bridle, S., Phys. Rev. D **66**, 103511 (2002) [arXiv:astro-ph/0205436].

Martinez, V. J., *et al.*, Astrophys. J. **696**, L93 (2009) [Erratum-ibid. **703**, L184 (2009)] [Astrophys. J. **703**, L184 (2009)] [arXiv:0812.2154 [astro-ph]].

Matsubara, T., Phys. Rev. D **77**, 063530 (2008) [arXiv:0711.2521 [astro-ph]].

Montesano, F.; Sanchez, A. G.; and Phleps, S., arXiv:1107.4097 [astro-ph.CO].

Okumura, T.; Matsubara, T.; Eisenstein, D. J.; Kayo, I.; Hikage, C.; Szalay, A. S.; and Schneider, D. P., Astrophys. J. **676**, 889 (2008) [arXiv:0711.3640 [astro-ph]].

Padmanabhan, N., *et al.* [SDSS Collaboration], Mon. Not. Roy. Astron. Soc. **378**, 852 (2007) [arXiv:astro-ph/0605302].

Padmanabhan, N.; Xu, X.; Eisenstein, D. J.; Scalzo, R.; Cuesta, A. J.; Mehta, K. T.; and Kazin, E., arXiv:1202.0090 [astro-ph.CO].

Peebles, P. J. E. 1980, The Large-Scale Structure of the Universe (Princeton, NJ: Princeton University Press)

Percival, W. J.; Cole, S.; Eisenstein, D. J.; Nichol, R. C.; Peacock, J. A.; Pope, A. C.; and Szalay, A. S., Mon. Not. Roy. Astron. Soc. **381**, 1053 (2007) [arXiv:0705.3323 [astro-ph]].

Percival, W. J., *et al.*, Mon. Not. Roy. Astron. Soc. **401**, 2148 (2010) [arXiv:0907.1660 [astro-ph.CO]].

Perlmutter, S., *et al.* [Supernova Cosmology Project Collaboration], Astrophys. J. **517**, 565 (1999) [arXiv:astro-ph/9812133].

Press W.H., Teukolsky S,A., Vetterling W.T., Flannery B.P., 1992, Numerical recipes in C. The art of scientific computing, Second edition, Cambridge: University Press.

Ratcliffe, A., et al., 1998, VizieR Online Data Catalog, 730, 417

Reid, B. A.; Percival, W. J.; Eisenstein, D. J.; Verde, L.; Spergel, D. N.; Skibba, R. A.; Bahcall, N. A.; and Budavari, T. *et al.*, Mon. Not. Roy. Astron. Soc. **404**, 60 (2010) [arXiv:0907.1659 [astro-ph.CO]].

B. A. Reid and M. White, arXiv:1105.4165 [astro-ph.CO].

Reid, B.A., et al., 2012, arXiv:1203.6641

Riess, A. G., *et al.* [Supernova Search Team Collaboration], Astron. J. **116**, 1009 (1998) [arXiv:astro-ph/9805201].

Sanchez, A. G.; Crocce, M.; Cabre, A.; Baugh, C. M.; and Gaztanaga, E., arXiv:0901.2570 [astro-ph].

Samushia, L.; Percival, W. J.; and Raccanelli, A., arXiv:1102.1014 [astro-ph.CO].

Seo, H., Eisenstein, D. J., 2003, ApJ, 598, 720

Smith, R. E., *et al.* [The Virgo Consortium Collaboration], Mon. Not. Roy. Astron. Soc. **341**, 1311 (2003) [arXiv:astro-ph/0207664].

Song, Y.-S.; Percival, W. J., 2009, JCAP, 10, 004

Song, Y. -S.; Sabiu, C. G.; Kayo, I.; and Nichol, R. C., JCAP **1105**, 020 (2011) [arXiv:1006.4630 [astro-ph.CO]].

Tegmark, M., *et al.* [SDSS Collaboration], Astrophys. J. **606**, 702 (2004) [arXiv:astro-ph/0310725].

Wang, Y., 2006, ApJ, 647, 1

Wang, Y., 2008, JCAP, 05, 021

Wang, Y., et al., MNRAS, 409, 737 (2010)

Wang, Y., 2012, MNRAS, 423, 3631

Wang, Y.; Chuang, C. -H.; and Mukherjee, P., Phys. Rev. D **85**, 023517 (2012) [arXiv:1109.3172 [astro-ph.CO]].

Xu, X., et al., 2012, arXiv:1206.6732

Zehavi, I., *et al.* [SDSS Collaboration], Astrophys. J. **621**, 22 (2005) [arXiv:astro-ph/0411557].